JRRD Volume 41, Number 3A, Pages 313–324
May/June 2004
Journal of Rehabilitation Research & Development

Application of adaptive filters to visual testing and treatment in acquired pendular nystagmus

Ryan M. Smith, BSEE; Brian S. Oommen, MS; John S. Stahl, MD, PhD
Departments of Neurology, Louis Stokes Cleveland Veterans Affairs Medical Center and Case Western Reserve University, Cleveland, OH

Abstract—Acquired pendular nystagmus (APN) complicates multiple sclerosis and other neurological disorders, causes visual impairment, and frequently resists treatment. Vision could be improved by a visual aid that gates or shifts the seen world in lockstep with the APN. Since the pathological oscillations are embedded in normal eye movements, such a device must track the nystagmus selectively. We evaluated the ability of an adaptive filter to perform this tracking and improve acuity when coupled to either of two devices—a shutter that permitted brief glimpses of the world synchronized with the nystagmus, or simulated image-shifting optics. In 10 normal subjects whose decimal acuity averaged 1.46 ± 0.20, acuity fell to 0.36 ± 0.08 under viewing conditions simulating APN. The synchronized shutter restored acuity to 0.60 ± 0.12, while image-stabilization raised it to 1.17 ± 0.13. Adaptive filters provide a practical means by which to track nystagmus. The most effective visual aid would couple such filters to image-stabilizing optics.

Key words: adaptive filter; adaptive optics; demyelination; liquid crystal; multiple sclerosis; nystagmus, pathological; optic neuritis; oscillopsia; shutter; visual acuity.

INTRODUCTION

Acquired pendular nystagmus (APN) is an involuntary, sinusoidal oscillation of the eyes that produces the illusion that the world is in motion (oscillopsia) and degrades the clarity of vision [1]. It affects approximately 3 percent of patients with multiple sclerosis [2,3] and is also seen occasionally as a complication of other disorders, particularly brainstem stroke [4,5]. APN is difficult to treat. While a large number of drugs have been reported to benefit selected patients, they are less satisfactory in general practice; many patients fail to respond to all agents or develop intolerable side effects such as sedation or ataxia [6–8]. Nonpharmacologic treatment strategies, including weakening selected extraocular muscles or using spectacle/contact lens combinations that optically negate the visual consequences of the oscillation have not gained wide patient acceptance [9,10]. One of the problems of the nonpharmacologic treatments is that they interfere with normal eye movements to the same extent that they attenuate or compensate for the pathological nystagmus. For instance, when using the spectacle/contact lens combination, the vestibulo-ocular reflex is nullified, and thus any head movements generate oscillopsia. Another problem specific to the spectacle/contact lens combination is that patients with APN are frequently too ataxic to insert a contact lens.

Abbreviations: APN = acquired pendular nystagmus, FLC = ferroelectric liquid crystal, LMS = least mean square.

This material was based on work supported by a Rehabilitation Research and Development award from the Department of Veterans Affairs.

Address all correspondence to Dr. John S. Stahl, Department of Neurology, University Hospitals of Cleveland, 11100 Euclid Avenue, Cleveland, OH 44106-5040; 216-844-3170; fax: 216-844-5066; email: jss6@po.cwru.edu.

The deficiencies of current treatments suggest a new therapeutic approach, i.e., a spectacle-mounted electronic/optical device that senses the patient's ocular oscillations and optically translates the image of the world to stabilize the image upon the moving retina. The device could potentially selectively track the involuntary oscillations, thereby avoiding the problem of interfering with the normal eye movements in which the oscillations are embedded. In a previous study, we investigated the feasibility of this treatment approach in five APN patients, using a prototype, table-mounted device in which the nystagmus was selectively tracked with analog electronics featuring a phase-locked loop circuit [11]. While the device improved acuity in most of the patients, the phase-locked loop design exhibited a number of insurmountable deficiencies, including its inability to respond to variations in the APN amplitude and the relatively long time required to achieve tracking lock after each interruption (typically three cycles of a patient's nystagmus). We suggested that these and other deficiencies could be corrected by replacing the phase-locked loop circuitry with a microprocessor-based adaptive filter.

In the current study we explored the use of an adaptive filter to track pendular nystagmus waveforms. The filter effectively adjusts the amplitude and phase of a sine wave so as to minimize the squared differences between that sine wave and the patient waveform (a so-called least-mean-square [LMS] algorithm [12]). In this way the filter generates a replica of the repetitive and undesirable sinusoidal component of the patient's eye movements. We used the sinusoidal filter output to control either an image-gating device or an image-shifting device, and assessed the efficacy of the system by determining its ability to restore acuity in normal subjects in whom the visual effects of APN were simulated by oscillating the acuity testing optotypes. The optotype oscillation was driven by either a sinusoidal waveform or an archived patient APN waveform.

An ideal APN treatment device would be lightweight, durable, easily worn/adjusted, and suitable for continuous use. A candidate device may fail to meet all these requirements and yet still be useful. For instance, a device that is too cumbersome for ambulatory use may still be helpful for reading or watching television. Even a device that is unsuitable for unsupervised patient use might still be employed in patient care. Many patients with APN due to multiple sclerosis have suffered optic neuritis, and as such their visual impairment reflects a combination of optic nerve injury and the nystagmus. An office-based APN device would allow the clinician to determine what a patient's acuity would be if the APN were successfully treated. Patients could be better counseled regarding the potential benefits of nystagmus treatments, and patients who would be unlikely to benefit could be spared extensive trials of the many medications that have been reported to benefit this disorder.

In the current study we explored the relative benefits of three different device configurations of ascending technical complexity. In the simplest arrangement, the subject viewed the oscillating acuity test pattern through a pair of shutters, which opened repetitively to give the subject very brief moments of vision. This arrangement generates a "stop-action" effect like that of a camera shutter. Such an arrangement would probably be suitable for brief use only (for instance, to read a sign) or as a tool of ophthalmologic assessment. Its major advantage is its simplicity—it requires only a pair of shutters and a simple circuit to gate and drive them. In the second arrangement, the subject viewed the pattern through the same shutters, and the adaptive filter was used to synchronize the shutter opening to the simulated nystagmus waveform. This arrangement is predicted to be more effective than the random shutter, because the acuity test optotypes "flash" at approximately the same position in the visual field (allowing the subject to align the direction of gaze with the optotype location). A synchronized shutter device would also be more complicated than the random shutter, in that it requires a continuous recording of the patient's eye movements as well as the microprocessor-based adaptive filter. In the third arrangement, the subject viewed the oscillating optotypes directly (i.e., without a shutter) under conditions that simulated the coupling of the adaptive filter to an image-shifting device capable of following the filter output with perfect fidelity. The third arrangement is predicted to generate the greatest benefit, as it affords continuous visibility of the visual world. However, a treatment device built along these lines would be the most complex, as it requires an eye movement sensor, the microprocessor-based adaptive filter, and the image-shifting optics and associated control circuitry.

METHODS

Subjects

Participating in this study were 10 normal subjects, aged 23 to 56 years. The experimental protocol was approved by the Institutional Review Board of the

Cleveland Veterans Affairs Medical Center, and all subjects gave informed consent. Subjects with optical correction wore that correction during testing.

Adaptive Filtering

The adaptive filter was modified from the adaptive interference canceler described by Widrow and Stearns [12] and implemented in Real-Time Simulink (The MathWorks, Natick, Massachusetts) on a Microsoft Windows 2000 platform. **Figure 1** diagrams the filter algorithm. The patient eye position (either horizontal or vertical) enters as a series of values $d(n)$, where n is the sample number. Three reference signals are also input, a constant value x_0 (set to 1.0), a cosine wave $x_1(n) = \cos(2\pi nf/N)$, and a sine wave $x_2(n) = \sin(2\pi nf/N)$, where N is the sampling rate of all the input signals in samples per second (fixed at 200 for these experiments) and f is the frequency of the pendular nystagmus in hertz. The reference signals are each multiplied by a different weight value, respectively $w_0(n)$, $w_1(n)$, and $w_2(n)$. The weighted sinusoids and constant are added together stepwise to generate $y_{012}(n)$ and $y_{12}(n)$, the filter outputs. $y_{012}(n)$ tracks all components of the eye movement, while $y_{12}(n)$ reflects only the pendular component. The filter error is calculated as $\varepsilon(n) = d(n) - y_{012}(n)$. For each time n, the weights for the next time point $n + 1$ are calculated as

$$w_0(n+1) = w_0(n) + 2\mu_0\varepsilon(n)x_0$$

$$w_1(n+1) = w_1(n) + 2\mu_1\varepsilon(n)x_1(n)$$

$$w_2(n+1) = w_2(n) + 2\mu_2\varepsilon(n)x_2(n)$$

μ_1 and μ_2 were set by trial and error to 0.1. Excessive μ values result in the $y_{12}(n)$ output following all components of the eye movement waveform. Insufficient values result in excessively long times to acquire tracking lock. The w_0x_0 input assures that, over time, $\varepsilon(n)$ is driven toward zero despite any sustained nonzero values in the eye position input, $d(n)$. μ_0 was set to 1/20 of μ_1. Insufficient values of μ_0 cause weights w_1 and w_2 to oscillate when mean eye position is nonzero. The oscillating weights do not actually degrade the ability of the output $y_{12}(n)$ to follow the APN component, but do render $\varepsilon(n)$ less useful as an index of whether the filter is in lock. Excessive values of μ_0 retard adaptation of w_1 and w_2, lowering the speed with which the filter responds to changes in APN amplitude or phase.

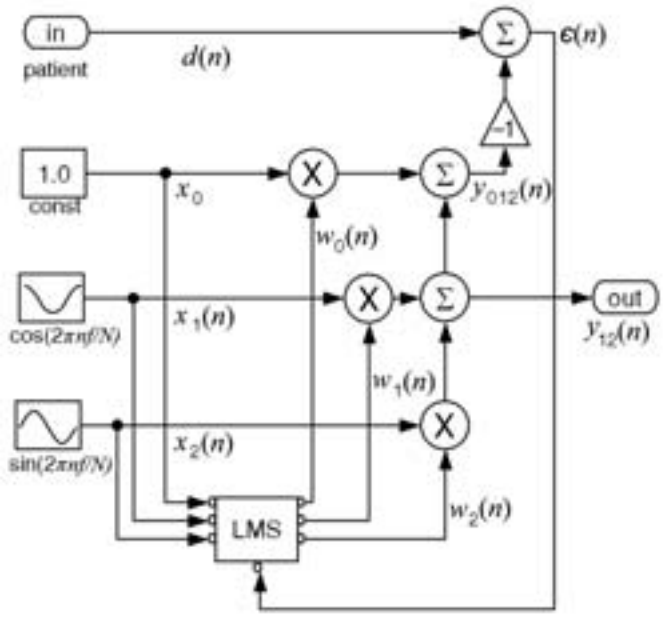

Figure 1.
Schematic description of adaptive interference canceller filter algorithm. LMS box adjusts values of weights w_0 to w_2 through least-mean-square procedure. All variables are defined in text.

The overall signal processing program used in the synchronized shutter testing is shown in simplified block form in **Figure 2a**. One dimension of eye position (horizontal or vertical, whichever exhibits the largest APN amplitude) is fed into the adaptive filter as $d(n)$. (Note that, ultimately, this input would come from an eye movement sensor incorporated in the device, but for the purposes of these experiments, the inputs were generated by the computer at a rate of 200 samples/s (see below)). The waveform is simultaneously passed through a block that determines f, the APN frequency. The block uses a fast Fourier transform to determine the frequency at which amplitude is maximal over the 3 to 8 Hz range, the usual range of APN [2–4,13]. In a given patient, APN frequency exhibits only minor variations over a timescale of minutes-days, so the frequency determination block provides a new estimate only once every 5 s. We wanted to open the shutter at a fixed point in each cycle of the nystagmus waveform, so we calculated the derivative of the filter output $y_{12}(n)$, used a comparator to determine when the derivative passed through 0 in the falling direction, and used the comparator output to trigger a 0.5 ms pulse. The pulse output then gated both shutters. The 0.5 ms duration was selected empirically, to provide the brightest

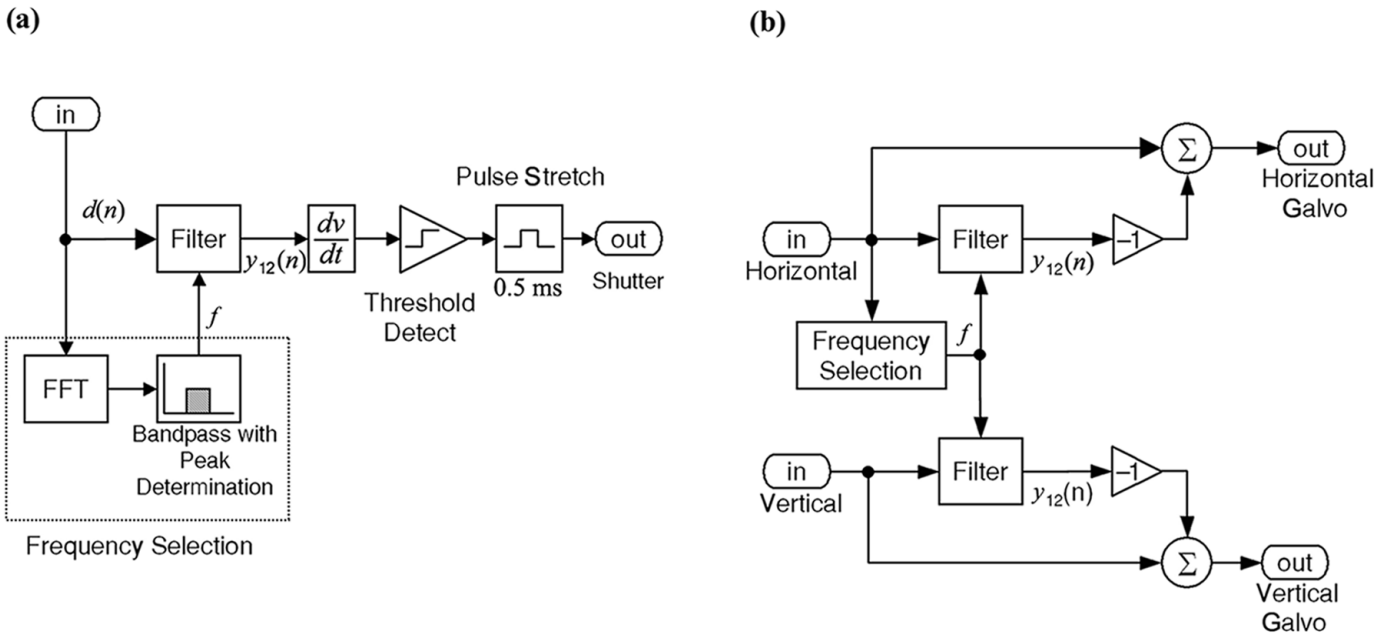

Figure 2.
Schematic description of implementation of filter algorithm in two treatment devices: (**a**) Circuit employed in shutter control. "Filter" box contains adaptive filter from **Figure 1**. (**b**) Circuit employed in simulated image-stabilization condition.

possible image while still preserving the "stop-action" effect of viewing through the shutters. For the purposes of these experiments, the normal subjects viewed the oscillating acuity optotypes binocularly, simulating the visual experience in a patient with identical nystagmus in both eyes. In patients, the nystagmus trajectories and amplitudes generally differ in the two eyes, and consequently separate tracking circuits would be required for each eye.

The circuit employed in the image-stabilization testing is shown in **Figure 2(b)**. For these experiments, both horizontal and vertical channels of the computer-generated eye movement were processed, using a pair of adaptive filter circuits. Since the oscillation frequency in different axes is almost always identical [2,14], the frequency determination block was included in only one channel. For these tests, each axis of the mirror galvanometer (see below) was driven by the difference between the horizontal or vertical component of the input waveform and the $y_{12}(n)$ output of the corresponding adaptive filter channel.

Visual Stimuli

Acuity testing optotypes consisted of white-on-black, eight-position Landolt C characters. Subjects were required to identify the orientation of the gap in each optotype. Pilot experiments revealed that subjects could often identify characters when projected singly, despite high degrees of motion blur. To solve this problem, the test optotype was presented as part of a 3 × 3 grid of characters, composed of the test optotype flanked by eight additional Landolt Cs, each oriented with the gap facing outward (see **Figure 3**). Intercharacter spacing on the grid was the same as that used in standard eye charts, i.e., characters were separated from each other by a one-character space. Adding the flanking characters to the stimulus better approximated what an APN patient would experience during reading, and sharply reduced the ability of normal subjects to identify the moving characters with the unaided eye. Test and flanking optotypes were scaled to range from 30 ft to 6 ft sizes in 0.1 logMAR steps. At our viewing distance of 10 ft, this range corresponds to decimal acuity chart sizes of 0.33 to 1.7, and a logMAR range of 0.48 to –0.23. Each test block consisted of a randomized set of 24 optotypes of a single size with each of the eight possible orientations occurring three times. During testing, each optotype was presented to the subject for 4 s. During transitions between optotypes, the old optotype first faded to black, and then a new character faded in.

Characters were designed in AutoCAD (Autodesk Inc., San Rafael, CA) and imported into Microsoft Powerpoint

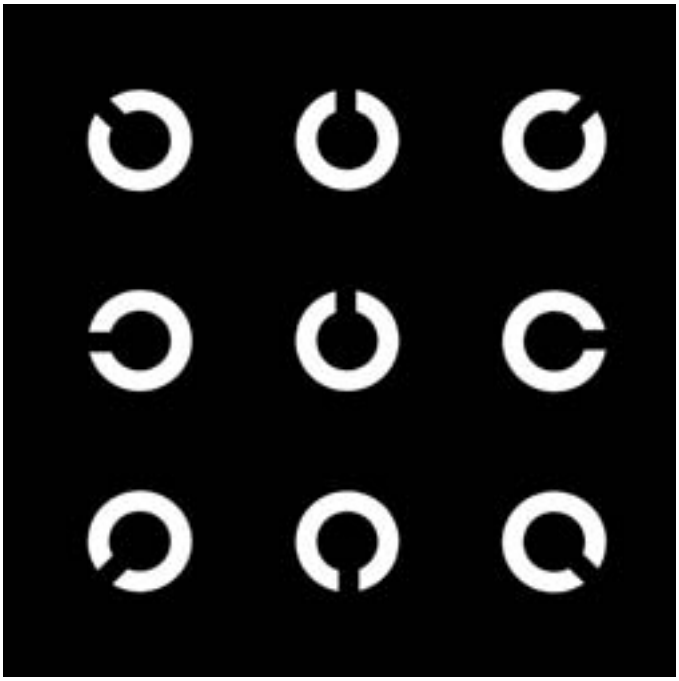

Figure 3.
Sample acuity testing pattern. Test optotype occupies center position and is surrounded by distractor optotypes.

for projection by a digital projector (model PJ550, ViewSonic) on a small white screen. The projected image had a luminance contrast ratio (light – dark)/(light + dark) of 0.97. The projection relayed through a pair of mirror galvanometers (model CX660, General Scanning), configured to deflect the image in horizontal and vertical directions. The deflection was driven in either of two trajectories. The first trajectory was circular, created by driving horizontal and vertical channels with a pair of 4.5 Hz, 1° amplitude (measured 0-peak) sinusoids in phase quadrature. This stimulus is, in some respects, a worst-case condition, as the optotype velocity is uniformly high. The second trajectory was created by driving the horizontal and vertical channels with an archived, 200 sample/s recording of eye movements of an actual patient whose nystagmus exhibited an elliptical trajectory with a cycle rate of 3.7 Hz and horizontal and vertical amplitudes of approximately 1.5° and 0.5°, respectively. We selected a 7.5 s record that was free of large saccades or large drifting movements (some of the latter probably representing reflex movements made to compensate for head movements). These non-APN movements would not be corrected by the shutter or image-shifting devices, and would thus interfere with vision in the normal subject. In contrast, they would not have troubled the patient who made them, as voluntary gaze-shifting and reflex gaze-stabilizing eye movements do not engender oscillopsia. The elliptical patient trajectory offers the viewer moments in which the optotype velocity is relatively low, but also introduces realistic noise components lacking in the circular trajectory.

Subjects viewed the acuity tests from a distance of 10 ft, under typical office fluorescent lighting conditions. During shutter testing, subjects viewed through a pair of FLC shutters (Ferroelectric Liquid Crystal Light Valves, Displaytech, Longmont, CO). The shutters are characterized by open and closed transmission rates of 29 percent and 0.024 percent, respectively, translating to an open:closed ratio of 1200:1. Since dark-adapted subjects could see through the closed shutter, dark adaptation was prevented by mounting the shutters in an open frame that admitted ambient lighting. Subjects viewed the projected acuity tests without the shutters when viewing stationary optotypes in the assessment of baseline acuity, and when viewing moving optotypes in the image-stabilized and "untreated" conditions (see below).

Experimental Procedure

We tested each subject using three different "treatment conditions." In the "random shutter" treatment condition, the shutter opened for a 0.5 ms period twice per second, with adjacent openings separated by random periods ranging from 0.1 to 0.9 s. In the "synchronized shutter" treatment condition, the shutter opened for 0.5 ms once per cycle of nystagmus, with the onset of the open period timed by the adaptive filter to occur near the minimum velocity point of the nystagmus component (horizontal or vertical) with the largest amplitude. In the "image-stabilized" treatment condition, the optotypes were oscillated under the control of the adaptive filter to simulate the image motion the subject would experience if the oscillating optotype were viewed through image-shifting optics capable of following $y_{12}(n)$ with great fidelity. Each treatment condition was evaluated with the use of the circular and/or patient-derived image motion trajectories, resulting in a battery of eight experimental conditions:

1. Circular trajectory viewed with the unaided eye ("circular trajectory, untreated")
2. Circular trajectory viewed through a randomly triggered shutter ("circular trajectory, random shutter")
3. Circular trajectory viewed through a synchronized shutter ("circular trajectory, synchronized shutter")

4. "Patient trajectory, untreated"
5. "Patient trajectory, random shutter"
6. "Patient trajectory, synchronized shutter"
7. Patient trajectory modified to simulate presence of high-fidelity image-shifting optics ("patient trajectory, image stabilized")
8. Stationary optotypes viewed with the unaided eye ("baseline acuity")

A ninth possible condition—circular trajectory with image stabilization—was not tested, as the resultant image was essentially indistinguishable from a stationary optotype. The battery required approximately 45 min to complete, and all subjects were tested twice, with testing sessions separated by at least one week. For each experimental condition, we began with larger character sizes and progressed to smaller sets until subject accuracy fell below 13/24 characters or, equivalently, 54 percent (the midpoint between perfect and chance performance). To further reduce the number of optotype sets we needed to test, we roughly identified the subset of sizes over which subject accuracy declined, with the help of a ranging set consisting of 5 characters of each size. The ranging could be performed for each of the 8 conditions, but in practice, performance across several of the conditions was usually similar, so only a few ranging operations were necessary. Subjects were given a brief rest between each stimulus condition. Subjects were instructed to indicate the orientation of each optotype as it displayed. The responses were entered into a Microsoft Excel spreadsheet, which automatically compared the responses to the correct sequence and tabulated the number of correct responses for each condition.

Data Analysis

Quantifying acuity in APN patients can be difficult with standard techniques, as there is often a large difference between the optotype size at which patients first begin to make errors, and the size at which they are unable to identify any optotypes correctly [11]. Accordingly, we substituted a procedure based on finding the size at which accuracy declines most sharply. To determine acuity for each subject and condition, we averaged the number of correct responses at each optotype size over the two testing sessions. We then plotted average number correct versus optotype size, expressing optotype size as it would appear on a decimal acuity chart, i.e., 5 ft letters at a viewing distance of 10 ft would correspond to a 2.0 line on a decimal acuity chart. We fit each accuracy curve with a three-term sigmoid $f(x) = a(1 + e^{-bx+c})^{-1}$, where x is optotype size, a is the maximum number of correct answers (24), and b and c are fitting variables. We then defined the subject's acuity for each condition as the value at which the fitted curve fell below our criterion level of 13 (see above). Where subjects did not reach the criterion, the sigmoid fit became unreliable. In those rare cases we linearly extrapolated from the closest two data points toward the criterion level, and defined the acuity as the point at which the extrapolated line crossed the criterion. Finally, we assessed the significance of *any* treatment effect using a two-way analysis of variance in which subject and visual conditions were the factors, and further compared the different conditions using the technique of planned comparisons between means [15]. Throughout, average values are given as mean ± standard deviation.

RESULTS

The adaptive filter exhibited robust tracking performance. **Figure 4** demonstrates the response to a simulated waveform containing a variety of transition conditions, including startup, saccades, and abrupt changes in nystagmus amplitude or phase, as well as a period of pursuit-like tracking. The top two traces show the pendular and nonpendular components from which the simulated waveform was composed. The third trace shows the composite simulated waveform ($d(n)$), with periods of shutter opening indicated by diamonds. The fourth and fifth traces show the sinusoidal filter output $y_{12}(n)$ and the reconstruction of the nonpendular component of the waveform calculated as $d(n) - y_{12}(n)$. Filter output matches the nystagmus perfectly over most of the record; track is reacquired following the interruptions within less than one-half cycle of the nystagmus waveform. The quality of the track is reflected in the degree to which the residual signal $d(n) - y_{12}(n)$ resembles the original eye position prior to addition of the pendular component. Shutter openings occurred at the proper point in the cycle, i.e., near the positive turnaround of the eye position signal.

Figure 5 shows waveforms, optotype trajectories, and filter responses used in subject testing. The performance with the pure sinusoid input is depicted in the left panels, while the performance with the patient waveform is shown on the right. Panels A1,A2 show the input waveforms and

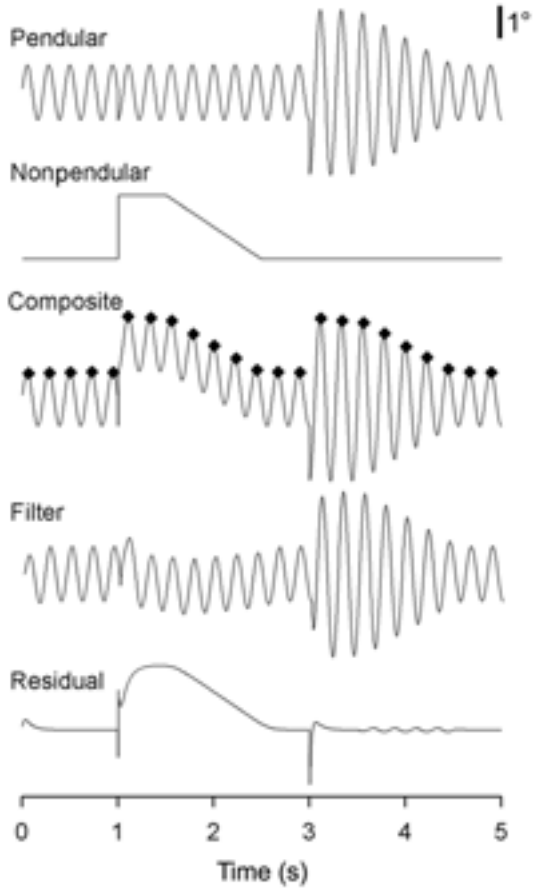

Figure 4.
Demonstration of filter tracking and shutter timing in response to artificial, single-axis eye movement waveform containing variety of perturbations. Patient waveform ($d(n)$, third trace) was created by adding pendular oscillation varying in amplitude and phase (first trace) to idealized series of eye movements. Fourth trace shows output ($y_{12}(n)$) of filter. Last trace shows difference between patient input and filter outputs, which is image motion a patient would experience while viewing through image-stabilization device. Solid diamonds in composite waveform indicate moments at which shutter opened in synchronized shutter condition.

the filter outputs $y_{12}(n)$ for the horizontal and vertical channels. The horizontal and vertical residual image motions ($d(n) - y_{12}(n)$) are also superimposed as thick lines on the input waveform plots. These residual motions are what would be experienced by an APN patient viewing through a high-fidelity image-shifting device driven by the $y_{12}(n)$ filter outputs, and it is these residual waveforms that are used to drive the mirror galvanometers in our simulated image-stabilized treatment condition. Panels B1,B2 and C1,C2 plot the vertical eye position versus horizontal eye position, and thus depict the trajectory of the optotype in the frontal plane. The moments of shutter opening are plotted as diamonds for the random shutter (B1,B2) and synchronized shutter (C1,C2) treatment conditions. The filter closely tracked the sinusoidal and patient input waveforms. In the random shutter condition, the optotype position at the moment of shutter opening was scattered over a broad region. Synchronized shutter opening greatly compressed the distribution of optoptype appearances. Thus in the synchronized condition the subject would be able to direct gaze to the location of optoptype appearance. In contrast, in the random condition it is impossible to predict the location of the appearance, and in many exposures the image of the optotype would fall entirely outside the retinal fovea.

Figure 6(a) shows the number of correct optotype identifications by one typical subject plotted as a function of optotype size (expressed as the level on a decimal acuity chart) for all stimulus conditions. All values represent the average of two sessions. For graphic clarity, lines connect the data points for each stimulus condition. **Figure 6(b)** replots the same data with the superimposed sigmoid fits. The dashed lines indicate the criterion and chance accuracy levels (13/24 and 3/24, respectively). In this example, there were too few data points to perform curve fitting for the patient waveform, untreated viewing condition; acuity was defined in this instance based on linear extrapolation, as described in METHODS. As in many of the subjects, acuity levels were ranked in the following descending sequence of conditions: (1) baseline acuity; (2) patient trajectory, image-stabilized; (3) circular trajectory, synchronized shutter; (4) patient trajectory, synchronized shutter; (5) patient trajectory, random shutter; (6) circular trajectory, random shutter; and (7) patient trajectory, untreated. In this as in all subjects, no optotypes could be identified in the remaining condition—circular trajectory, untreated. This condition is excluded from the figure.

Table 1 gives the acuity values for all 10 subjects in the 7 informative conditions, and **Figure 7** plots the corresponding means and standard deviations for the tabulated data. As before, the circular trajectory, untreated condition was excluded, as no subject was able to identify any optotypes with the largest size we tested. As predicted, the image-stabilized condition approached baseline acuity most closely. The efficacy in the random and synchronized shutter treatments (operating upon the patient trajectory stimulus) was significantly lower than in the image-stabilized treatment condition (both comparisons $p < 0.001$), and the random shutter was inferior

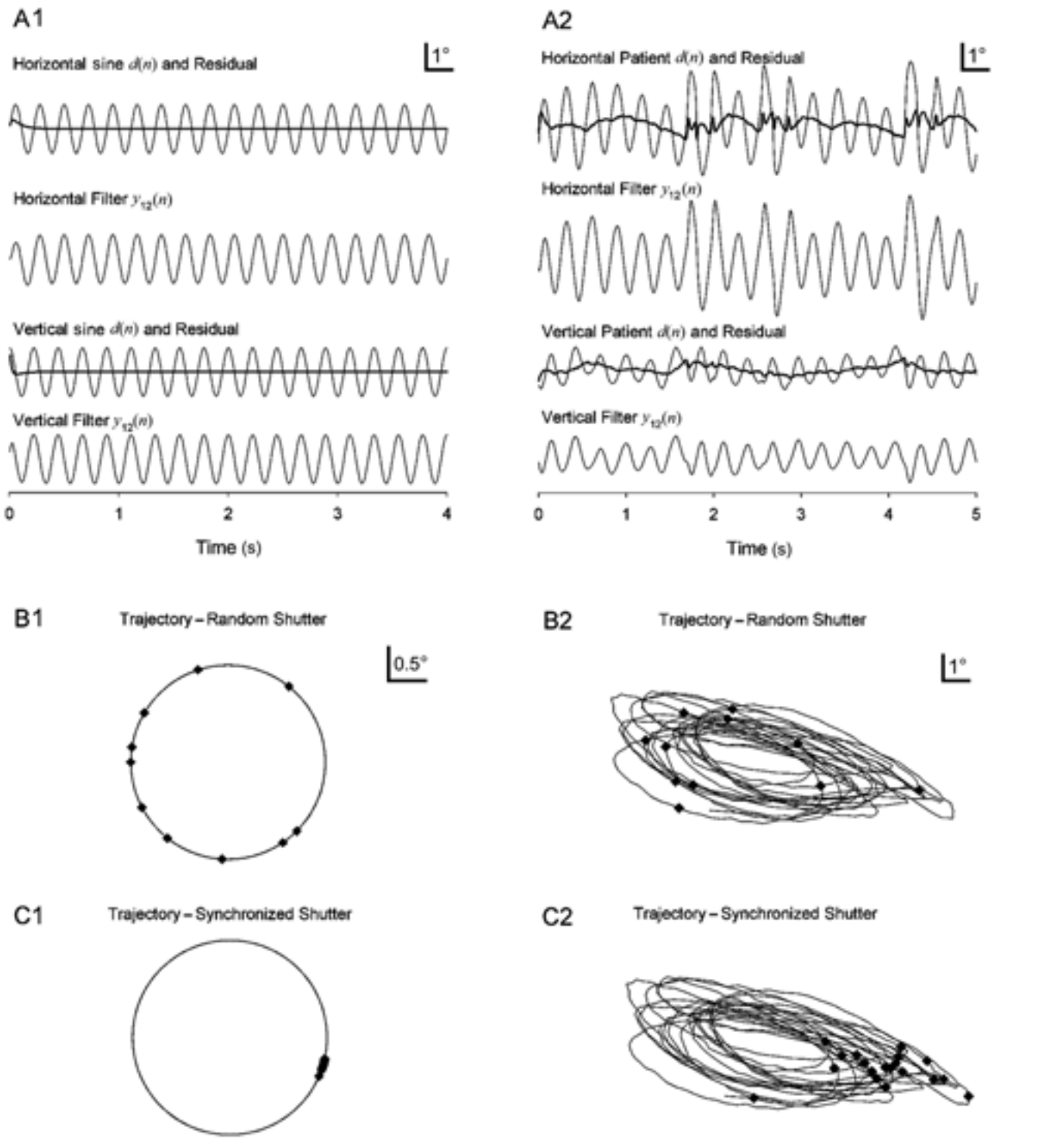

Figure 5.

Time and trajectory plots of system response to sinusoidal (left column) and patient waveform (right column) inputs. A1,A2: Plots of horizontal and vertical eye position, as well as horizontal and vertical filter outputs ($y_{12}(n)$) versus time. Residual image displacement ($d(n) - y_{12}(n)$) is superimposed on patient waveforms (thick lines). B1,B2: trajectory of optotype image in frontal plane. Diamonds indicate moments of shutter opening in random shutter condition. C1,C2: same as B1,B2, except shutter openings reflect synchronized shutter condition. Note that B and C panels share scales, but scales for B1,C1 differ from those of B2 and C2.

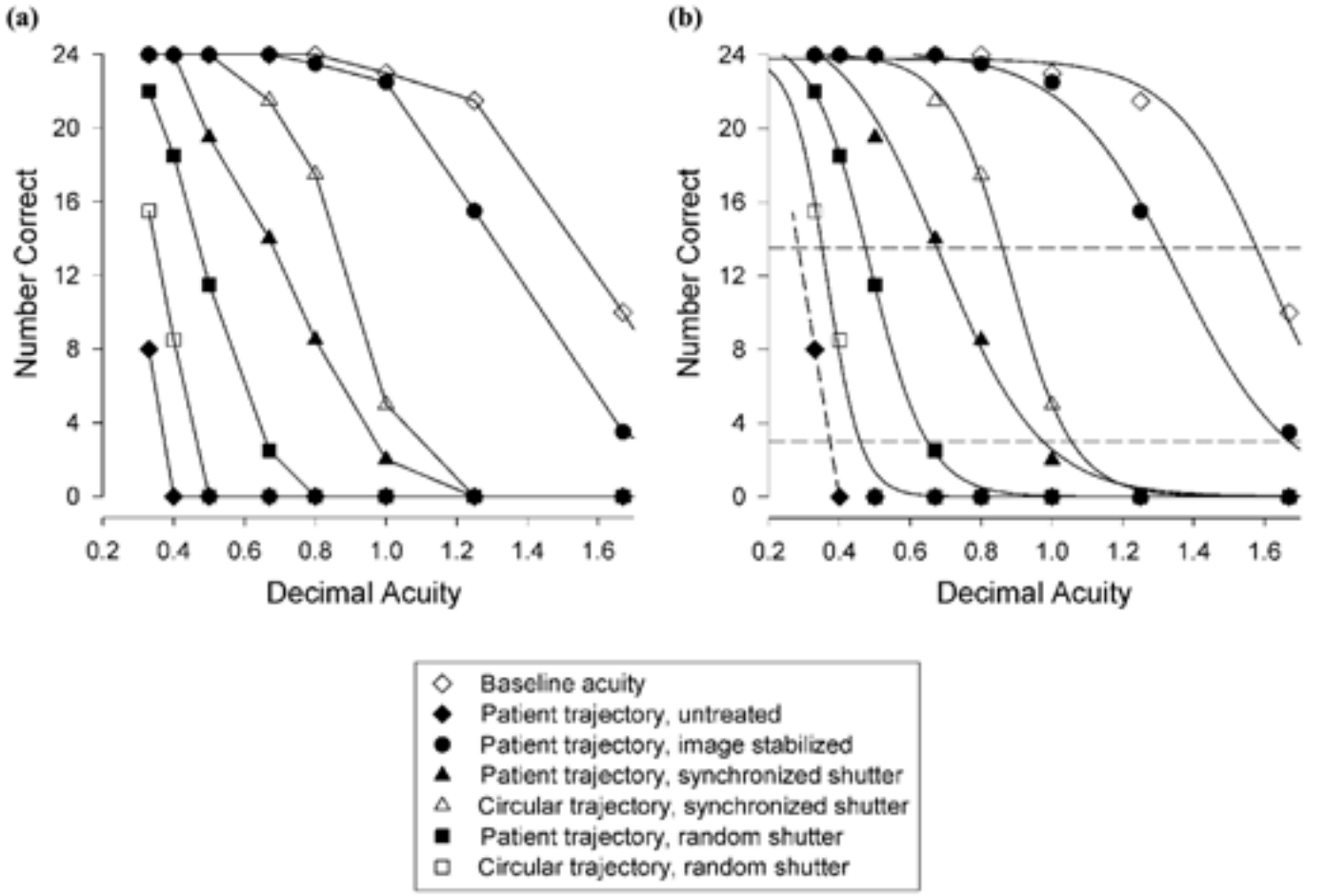

Figure 6.
Plots of number of correctly identified optotypes as functions of optotype size for one subject (average of two measurement sessions). Scores from each of seven informative conditions are plotted using different symbols (see key). **(a)** Scores from each condition are connected by straight lines for graphic clarity. **(b)** Same as **(a)**, except straight lines are replaced by sigmoid fitted curves as described in text. Dashed lines indicate chance and criterion performance levels. Acuity for each condition was defined as optotype size at which fitted curve crossed criterion line.

to the synchronized shutter (p = 0.001). Although mean acuity in the patient trajectory, random shutter condition was greater than in the patient trajectory, untreated condition, the difference was not statistically significant (p = 0.13). We could not quantify the analogous comparison for random shutter and untreated (naked-eye) viewing of circular trajectories, as the latter acuity was off-scale low. Presumably the difference would have been significant, as all subjects could identify some characters using the random shutter, but no subjects could identify any characters when viewing the circular trajectory with the naked eye.

Inspection of the mean acuities in the shutter treatments reveals an interesting contrast. On one hand, with the random shutter, acuity with the patient trajectory was superior to the circular trajectory. On the other hand, with the synchronized shutter, acuity with the patient trajectory was inferior to the circular trajectory. While the differences in the means were not statistically significant, the pattern probably is physiologically meaningful, as it is easily explained with reference to the trajectories depicted in **Figure 5**. For the random shutter treatment, the positions of shutter openings are clustered more tightly in the patient trajectory than in the circular trajectory, a reflection of the smaller area covered by the former trajectory. In contrast, in the synchronized condition, shutter openings are clustered more tightly in the circular trajectory, a reflection of the fact that the patient trajectory contains noise components that are not tracked by the adaptive filter.

Table 1.
Acuity values for all 10 subjects in the seven informative experimental conditions.

Subject	Baseline	Patient, Stabilized	Circular, Synchronized Shutter	Patient, Synchronized Shutter	Circular, Random Shutter	Patient, Random Shutter	Patient, Untreated
S1	1.273	1.197	0.652	0.456	0.300	0.341	0.320
S2	1.572	1.321	0.861	0.688	0.351	0.476	0.300
S3	1.340	1.014	0.625	0.566	0.379	0.447	0.290
S4	1.707	1.284	0.662	0.555	0.286	0.346	0.358
S5	1.251	1.001	0.662	0.579	0.342	0.431	0.356
S6	1.296	1.057	0.718	0.571	0.314	0.468	0.300
S7	1.750	1.305	0.817	0.645	0.332	0.496	0.305
S8	1.352	1.037	0.940	0.808	0.315	0.554	0.426
S9	1.697	1.184	0.544	0.421	0.285	0.295	0.383
S10	1.404	1.273	0.681	0.725	0.415	0.477	0.553

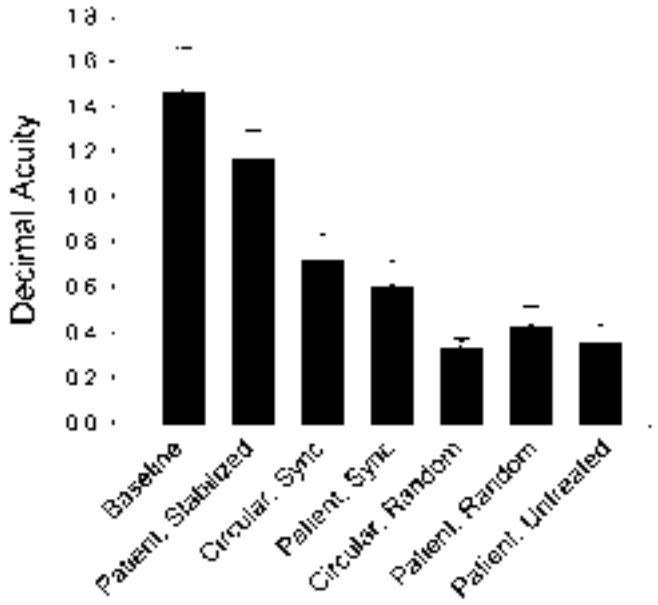

Figure 7.
Average acuity values in seven informative conditions for all subjects. Error bars represent ±1 standard deviation.

DISCUSSION

The digital adaptive filter resolved many of the deficiencies we identified in the analog tracking circuitry employed in our earlier prototype APN treatment device [11]. It was capable of reestablishing tracking lock rapidly following a variety of transition conditions. Unlike our earlier phase-locked loop circuit, it was also capable of following variations in nystagmus amplitude. Converting from analog electronics to software-based instrumentation also greatly accelerated the development process, and will facilitate the development of additional features required in a practical treatment device, such as patient-friendly controls, or the ability to detect the out-of-lock condition (so that the shutter or image-stabilizing optics can be disabled when their motion would not improve vision). The digital platform also facilitates investigating different tracking algorithms for use in treating nonsinusoidal oscillations. While our software was implemented on a desktop computer, it can eventually be shifted to a belt-mounted control unit, using Real-Time Simulink's support for embedded microprocessors.

As demonstrated using simulated complex eye movement waveforms, the adaptive filter exhibited the necessary ability to track the sinusoidal nystagmus waveform despite its being embedded in other eye movements. That selectivity, however, is not complete. Using our selected values of μ_0, μ_1, and μ_2, and a center frequency f of 4.5 Hz, the filter exhibits 50 percent attenuation or greater over a frequency range of approximately 3.0 to 6.5 Hz and 30 percent attenuation or greater over 2.5 to 8.5 Hz. Thus the filter is expected to interact with normal eye movements to the extent that their power spectra coincide with this range. Such movements would include those made in response to natural head rotations (i.e., vestibulo-ocular reflex movements), since natural head movements have predominant frequencies in the 0.5 to 5.0 Hz range [1]. Interference with the vestibulo-ocular reflex might be reduced by including an angular accelerometer in the head-mounted portion of

the device, and using its output to deduct a predicted vestibulo-ocular reflex eye movement from the total eye movement signal prior to its being input to the adaptive filter. Determination of the significance of this problem must await the development of a complete device suitable for testing during natural behaviors such as sitting, standing, and walking.

Patients may have other, nonpendular components to their APN. A jerk component is common, and in our previous study, may have contributed to one patient failing to benefit from the device [11]. It remains unknown whether jerk and pendular components are driven by the same pathological oscillator. It is conceivable that the jerk nystagmus reflects a constant eye velocity bias (as opposed to an oscillation) that visual mechanisms of gaze stabilization would be capable of suppressing, were it not for the high retinal image velocities engendered by the concomitant pendular oscillation. In that case, the jerk component may vanish if the pendular component were sufficiently countered by an image-stabilizing treatment device. This practical question, as well as a larger theoretical issue of the extent to which the nystagmus waveform can be altered by changing visual feedback, must await experiments in APN patients using the adaptive filter and actual image-shifting optics.

Indeed, the extent to which the simulated image-stabilizing condition out-performed the FLC shutters indicates that realization of an APN treatment device will absolutely require developing practical, high-fidelity image-shifting optics. Our previous prototype device accomplished image shifting using a pair of cascaded Risley prisms [11]. The device exhibited rather poor fidelity, and in addition, was inherently difficult to miniaturize or render suitable for continuous, battery-powered operation. Fortunately, an improved device is definitely feasible, as evidenced by the existence of consumer products such as binoculars and photographic lenses with built-in image-stabilization. Some of these products rely on variable-power prisms, while others utilize lens combinations that shift the image when one of the lens elements is translated in a plane perpendicular to the optical axis. It should be noted that all of these mechanisms are designed to compensate for horizontal and vertical perturbations only, and thus would not be sufficient to treat an APN patient with strong torsional components. Treating torsional components of nystagmus is also problematic because the eye movement sensor technologies that would be applicable to an APN treatment device (e.g., electrooculography, infrared reflectance, or, the most economical, video-based pupil trackers) cannot transduce the torsional motion.

While inferior to the simulated image stabilizer, the FLC shutters were still superior to naked-eye viewing. As noted in the introduction, they might find a role for brief use to read large print, or as a tool to evaluate acuity during ophthalmologic examinations. They would presumably be more useful in patients in whom the nystagmus cycle includes periods of near stationarity (for instance, in a patient with single-axis nystagmus, in which case image velocity falls to zero twice in each nystagmus cycle). In such cases the shutter opening duration could be increased above the 0.5 ms value used in our experiments, yielding a subjectively brighter image. Note that we purposely chose test waveforms in which the image velocity was continuously high, requiring us to use a short shutter opening period in order to generate the “stop-action” effect. It should also be noted that luminance was quite high in our projected acuity charts. We did not investigate visual function using printed acuity characters, which would more closely model the luminances experienced by a patient attempting to read. The current study was also limited to testing the ability of subjects to identify single optotypes, albeit when embedded in a matrix of additional characters. Further evaluation of a shutter-based visual aid must include an assessment of the ability of patients to read complete words when viewing through shutters.

CONCLUSIONS

A digital adaptive interference filter can selectively track pathological sinusoidal eye movements, while ignoring concomitant normal eye movements. Such a filter could serve as the tracking element of a visual aid for patients suffering from APN. The greatest benefit is expected from a device in which the filter drives adaptive optics that stabilize the visual world on the moving retina. However, some benefit is also derived when the filter drives a simpler shutter device that permits a tachistoscopic view of the world that is synchronized to the nystagmus waveform. A computer-controlled device that permits the visual world to be shifted in response to movements of a patient’s eyes has applications to treatment, evaluation, and basic research in patients with involuntary ocular oscillations.

ACKNOWLEDGMENTS

The corresponding author is indebted to Paul Dean and Lance Optican, who directed him to the Widrow and Stearns reference and the adaptive filter technique it describes.

REFERENCES

1. Leigh RJ, Zee DS. The Neurology of Eye Movements. 3rd ed. New York: Oxford University Press; 1999.
2. Aschoff JC, Conrad B, Kornhuber HH. Acquired pendular nystagmus with oscillopsia in multiple sclerosis: a sign of cerebellar nuclei disease. J Neurol Neurosurg Psychiatry. 1974;37:570–77.
3. Barton JJ, Cox TA. Acquired pendular nystagmus in multiple sclerosis: clinical observations and the role of optic neuropathy. J Neurol Neurosurg Psychiatry. 1993;56:262–67.
4. Gresty MA, Ell JJ, Findley LJ. Acquired pendular nystagmus: its characteristics, localising value and pathophysiology. J Neurol Neurosurg Psychiatry. 1982;45:431–39.
5. Nakada T, Kwee I. Oculopalatal myoclonus. Brain. 1986; 109:431–41.
6. Averbuch-Heller L, Tusa RJ, Fuhry L, Rottach KG, Ganser GL, Heide W, et al. A double-blind controlled study of gabapentin and baclofen as treatment for acquired nystagmus. Ann Neurol. 1997;41:818–25.
7. Leigh RJ, Averbuch-Heller L, Tomsak RL, Remler BF, Yaniglos SS, Dell'Osso LF. Treatment of abnormal eye movements that impair vision: strategies based on current concepts of physiology and pharmacology. Ann Neurol. 1994;36:129–41.
8. Stahl J, Averbuch-Heller L, Leigh R. Acquired nystagmus. Arch Ophthalmol. 2000;118:544–49.
9. Leigh RJ, Tomsak RL, Grant MP, Remler BF, Yaniglos SS, Lystad L, et al. Effectiveness of botulinum toxin administered to abolish acquired nystagmus. Ann Neurol. 1992;32: 633–42.
10. Rushton D, Cox N. A new optical treatment for oscillopsia. J Neurol Neurosurg Psychiatry. 1987;50:411–15.
11. Stahl JS, Lehmkuhle M, Wu K, Burke B, Saghafi D, Pesh-Imam S. Prospects for treating acquired pendular nystagmus with servo-controlled optics. Invest Ophthalmol Vis Sci. 2000;41:1084–90.
12. Widrow B, Stearns SD. Adaptive signal processing. Upper Saddle River, New Jersey: Prentice-Hall; 1985.
13. Lopez LI, Bronstein AM, Gresty MA, Du Boulay EPG, Rudge P. Clinical and MRI correlates in 27 patients with acquired pendular nystagmus. Brain. 1996;119:465–72.
14. Barton JJ. Is acquired pendular nystagmus always phase locked? J Neurol Neurosurg Psychiatry. 1994;57:1263–64.
15. Sokal RR, Rohlf FJ. Introduction to biostatistics. 2nd ed. New York: W. H. Freeman; 1987.

Submitted for publication March 27, 2003. Accepted in revised form August 12, 2003.